IEEE Access
Multidisciplinary | Rapid Review | Open Access Journal

Received August 3, 2020, accepted September 10, 2020, date of publication September 18, 2020,
date of current version September 30, 2020.

Digital Object Identifier 10.1109/ACCESS.2020.3024712

Triboelectric Self-Powered Three-Dimensional Tactile Sensor

ZHIHUA WANG[1,2], SHIMING SUN[1,2], NA LI[3], TAO YAO[4], AND DIANLI LV[1,2]

[1]State Key Laboratory of Reliability and Intelligence of Electrical Equipment, Hebei University of Technology, Tianjin 300130, China
[2]Key Laboratory of Electromagnetic Field and Electrical Apparatus Reliability of Hebei Province, Hebei University of Technology, Tianjin 300130, China
[3]Industrial Technology Center, Chengde Petroleum College, Chengde 067000, China
[4]School of Mechanical Engineering, Hebei University of Technology, Tianjin 300130, China

Corresponding author: Zhihua Wang (wangzhihua@hebut.edu.cn)

This work was supported in part by the National Natural Science Foundation of China under Grant 51775166, and in part by the Hebei Province Foundation for Recruiting Returned Scholars under Grant CL201708.

ABSTRACT Three-dimensional tactile sensing in smart devices is witnessing an increasing demand. In this study, a three-dimensional tactile sensor is proposed according to the principle of triboelectricity by using polydimethylsiloxane (PDMS) and polyethylene oxide (PEO) films. Use of PDMS-ZnO composite films increases the output voltage of the electrodes. The sensor is designed with a cross beam-shaped pressure head to enable sensing normal forces in five directions. The working mechanism of the sensor is analyzed using the finite element method. The calculation results indicate a linear relationship between the output voltage and the force. The simulation results also demonstrate that the output voltage is linearly correlated with the applied force in the range of 1-30 N. Test results show that the sensor can sense the magnitude, frequency, and direction of the force as well as measure the duration of the force. The hardness of the object has a significant effect on the output voltage. Finally, the sensor is tested on a manipulator grasping an object to demonstrate its ability to sense the contact and sliding of the object.

INDEX TERMS PDMS, PEO, sliding sensing, three-dimensional tactile sensation, triboelectricity.

I. INTRODUCTION

With the advancement of technology and increasing demand for convenient living, human-computer interaction is gaining increasing application and the intelligent robot industry has achieved unprecedented development. Consequently, tactile sensation, an important method for robots to sense the external environment, has become an indispensable ability for intelligent robots [1]. Tactile sensors convert tactile signals into electrical signals, which are easily transmitted to the central controller. Tactile sensors currently in use are mainly capacitive [2], [3], resistive [4], [5], and piezoelectric [6]. They generally detect touch pressure in one direction [7]. However, smart robots need rich tactile information, including information on three-dimensional force [8], such as normal force and tangential force, as well as object motion, displacement, and temperature [9]. Among them, slip detection is important information for a robot to stably grasp objects, especially flexible objects. The flexible tactile sensor array made of conductive rubber has the ability to detect distributed contact force and sliding [10]. A large-area, fully-flexible tactile sensor array is developed with 12 units that can so as to cover the entire palm. And 2 to detect robotic hand grasping forces to get slippage.for determining slip. However, this sensor array is characterized withby relatively lower sensitivity and spatial resolution [11]. Therefore, developing sensors with multiple tactile sensing capabilities is of great importance.

Traditional sensors usually require external power or batteries, which hinders the development of economic, portable, and environmentally sustainable sensors. To solve this problem, self-powered sensors [12] can be developed by taking advantage of triboelectric, piezoelectric [13], [14], and pyroelectric [15] effects. Through the stimulation of environmental changes such as external mechanical vibration or pressure, the corresponding electrical signals are generated through sensitive materials [16] to achieve tactile perception. In 2006, Wang Zhonglin *et al.* first proposed a piezoelectric nanogenerator based on zinc oxide (ZnO) nanomaterials [17]. A triboelectric nanogenerator, which combines the triboelectric effect and electrostatic induction, is a new type of electro-mechanical converter [18]. When this nanogenerator

The associate editor coordinating the review of this manuscript and approving it for publication was Kin Kee Chow.

is subjected to mechanical deformation, it generates voltage signals and can sense the dynamic force. A research showed that polydimethylsiloxane (PDMS), polyvinylidene fluoride (PVDF), and polytetrafluoroethylene (PTFE) have strong electronic affinity and are excellent highly negative triboelectric materials [19]. In general, metals such as copper, silver, and gold are used as the electropositive materials. However, when polyethylene oxide (PEO) is used as the electropositive material, a charge density of 154 μC/m^2 and a peak power of 4 W/m^2 are achieved; the power thus achieved is higher than that of nanogenerators that use metal electrodes [20]. For the applications as E-skin, significantSignificant breakthroughs have been achieved in TENGs the application of triboelectric nanogenerator sensors ofas electronic skin with high sensitivity, high spatial resolution, and large scale. Through theoretical analysis and experimental studies, Lin *et al.* demonstrated that TENGs couldthe function of triboelectric nanogenerators as effective pressure sensors for detection ofto detect both static and dynamic external loads [21]

In this study, a new three-dimensional tactile sensor is designed on the principle of triboelectric charging. PEO is used as the electropositive material, PDMS is used as the electronegative material, and nanometer ZnO powder is doped in PDMS. The sensitive materials used herein are softer than PVDF and the other piezoelectric materials and can sense low pressure [22]. The proposed sensor has better linearity and sensitivity under low pressure [23]. The COMSOL software is used to simulate the three-dimensional tactile sensor and analyze the potential distribution and change law.

The proposed sensor can comprehensively perceive signals corresponding to complex external stimuli such as pressing, touching, and vibration, and it shows better environmental adaptability than the pure pressure-sensing sensor [24]. The sensor can be self-powered without the need for an external power source and can sense normal and tangential forces, recognize sliding of objects, and judge the degree of softness and hardness of an object. Moreover, the sensor has good linearity, reliability and robustness. The sensitivity is 46mv46 mv/N, and the linear correlation coefficient R2 is 0.9914. Consequently, the sensor has an extensive application value in the fields of intelligent robots, health monitoring, and human-computer interaction.

II. FILM FABRICATION AND SENSOR DESIGN

A. PEO FILM FABRICATION

A PEO solution with 10% mass fraction was prepared by dissolving 10 g of PEO (Ryoji Organic Chemical) powder having a molecular weight of 600,000 in 90 g of deionized water and subjecting the mixture to magnetic stirring for 2 h till the PEO powder is completely dissolved. Then, the PEO solution was spin-coated on a glass plate to a thickness of 100 μm using a molding machine; the PEO-coated glass plate was placed in a drying box and dried at 70 °C for 30 min to prepare a dense PEO film.

B. PDMS FILM FABRICATION

A mixture of 50 g PDMS A solution and 5 g PDMS B solution was prepared at a mass ratio of 10:1 and stirred with a magnetic stirrer for 1 h. The PDMS (184 Silicone Elastomer, Dow Corning Co. Ltd.) solution was divided into two parts. One part is left to stand for one hour to remove bubbles. To the other part, 5 g of ZnO (Shanghai Chaowei Nano Technology Co. Ltd.) powder of particle size 200 nm was added and stirred thoroughly to prepare a PDMS solution with 10% mass fraction of ZnO; this solution was then let to rest for 1 h to remove bubbles before using it to make PDMS-ZnO films. Both types of PDMS solutions were spin-coated on glass plates to a thickness of 140 μm and dried in a drying box at 70 °C for 1 h to prepare the PDMS and PDMS-ZnO films. Electron microscopy of the PDMS-ZnO film was performed, as shown in Fig. 1. White particles observed on the surface of the film show good dispersibility in PDMS with relatively uniform size and no obvious agglomeration. Spectroscopic analysis of the PDMS-ZnO film confirms the presence of zinc (Fig. 2(a)).

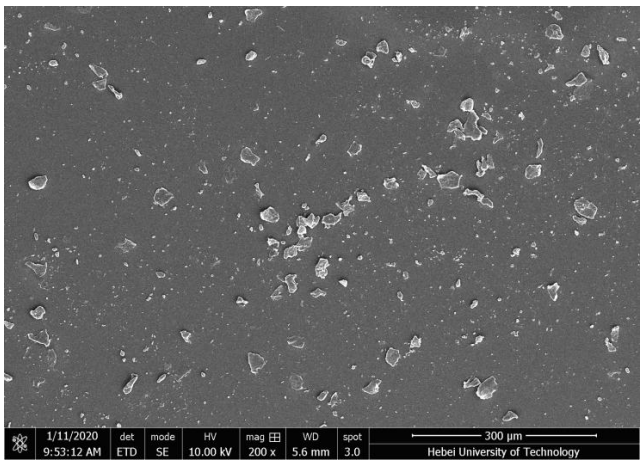

FIGURE 1. Electron microscopy of PDMS-ZNO film.

C. SENSOR DESIGN AND FABRICATION

The sensor is an open hollow cube with dimensions 13 mm × 13 mm × 13 mm and thickness 2 mm (Fig. 2(b) and Fig. 2 (c)). A cross beam-shaped pressure head that is made of 12% mass fraction PDMS solution by an inverted mold technology is first placed in the middle of the hollow cube, just touching its bottom. Second, a certain amount of 10% PDMS solution is dropped onto the connection between the pressure head and the hollow cube. Finally, the pressure head is fixed after PDMS curing. The pressure head is located 2 mm away from the inside of the cube. When a tangential (Fig. 2(d)) or a normal (Fig. 2(e)) force is applied to the cross beam-shaped pressure head, the inside of the cube will be squeezed, causing the two film layers to come in contact and generate friction. The corresponding electrical signal is output owing to the triboelectric effect and electrostatic induction. PDMS is an electronegative material and easily

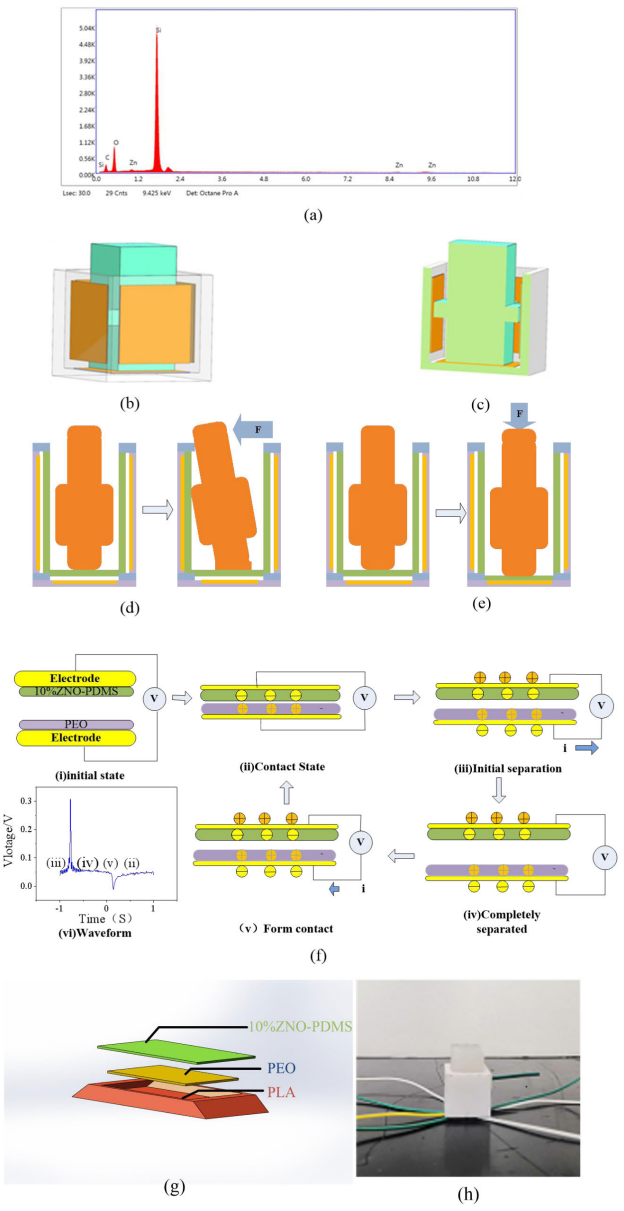

FIGURE 2. Energy spectrum diagram (a) of the PDMS-ZnO film; 3D exterior (b) and interior (c) views; schematic diagrams of tangential (d) and normal (e) forces applied on the pressure head, and the charge transfer process of the sensor (f); installation diagram of the PEO and PDMS-ZnO films (g); and the photo of the prototype (h).

gains electrons, while PEO is an electropositive material and easily loses electrons. The charge transfer process of the sensor is shown in Fig. 2(f). As the external pressure causes the PDMS-ZnO and PEO films to come into contact with each other, a positive charge is induced on the upper layer of the PDMS-ZnO film and a negative charge is induced on the lower layer of the PEO film, thereby generating a positive electromotive force (EMF). Due to the high impedance characteristics of PMDS-ZnO and PEO films, charges will remain on the film surfaces. Before the two films are separated, the potential difference between the upper and lower electrodes is zero. Immediately after the separation of the two charged films, an electric field is formed between the film surfaces, thereby causing a negative potential difference between the electrodes. After the PDMS-ZnO and PEO films are completely separated, the electrostatic equilibrium is reached again. The test voltage waveform in Fig. 2(f) reflects the changes in the EMF during the contact-separation process of the PDMS-ZnO and PEO films.

The outer frame of the sensor is made by 3D printing with polylactic acid (PLA) material. Two membranes are placed on the inside of five faces of the cube. On each side of the PEO film and the 10% ZnO-PDMS film, a nickel-plated copper conductive non-woven fabric is pasted and the wires are led out. The side of the PEO film from which the lead wire comes out is attached to the inside of the sensor, and the 10% ZnO-PDMS film covers the PEO film, as shown in Fig. 2(g). The outer and inner layers are a PEO film and a PDMS-ZnO film, respectively, both having an area of 9 mm × 9 mm, with a 1 mm gap between them. The prototype is shown in Fig. 2(h).

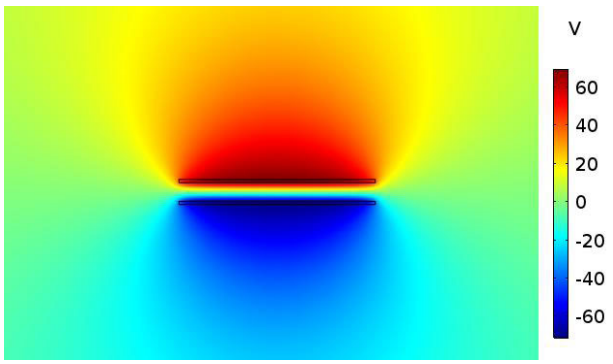

FIGURE 3. Potential distribution when the PDMS and PEO films are separated.

III. EXPERIMENTS AND RESULTS

A. SIMULATION

The COMSOL software was used to simulate the potential distribution of the sensor during the contact and separation of the PDMS-ZnO and PEO films. The PDMS-ZnO film with a surface charge density of 154 μC/m^2 and the PEO film with a surface charge density of -154 μC/m^2 were set as the upper and lower layers, respectively. The simulation diagrams (Figs. 3 and 4) indicate that as the distance between the electrodes gradually increases, the potential increases. The finite element calculation shows a linear relationship between the voltage and the distance between the films (Fig. 5). This is because when the two triboelectric materials come into contact, electron transfer occurs owing to the difference in the attraction of the two triboelectric materials to charge. In addition, when the triboelectric materials gradually separate, owing to electrostatic induction, the electron flow in the electrode on the back of the triboelectric material and the potential gradually increase until the triboelectric material becomes electrically neutral. Fig. 6 shows

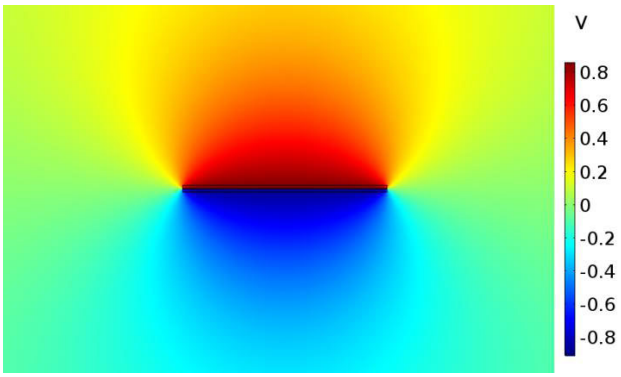

FIGURE 4. Potential distribution when the PDMS and PEO films are in contact.

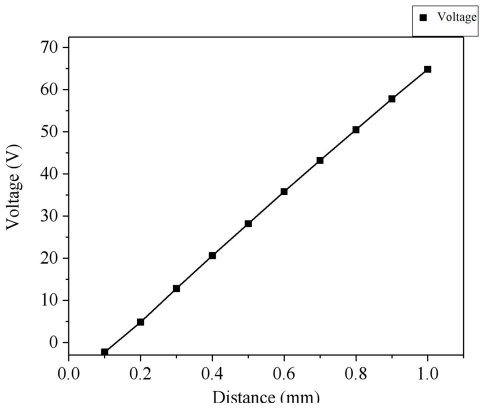

FIGURE 5. Relationship of the distance between the two films and the output voltage.

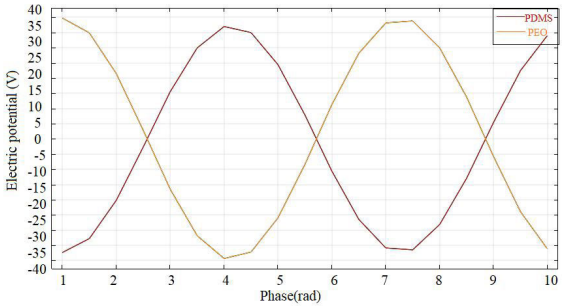

FIGURE 6. Phase changes of the potentials of the upper and lower layers.

the phase relationship between the potentials of the upper and lower layers. The potential difference waveform is consistent with the measured output voltage waveform of the sensor. The surface of the PDMS-ZnO and PEO films are positively and negatively charged, respectively, when they are in contact. The potentialdifference between the two films is positive, which becomes zero after stable contact is achieved. Further, immediately after the separation of the two films, a negative potential difference occurs. These potential changes follow the electrical principle of power generation by friction.

B. COMPARISON OF PDMS AND PDMS-ZNO FILMS

A signal generator was used to provide a 1 Hz sinusoidal signal to the vibration modal analyzer. The output voltage of the power amplifier was adjusted to control the output force of the vibration motor. Further, a force ranging 1–30 N was applied at 1 Hz on the pressure head of the sensors made with the PDMS film and PDMS-ZnO film, separately. The PDMS solution with 5%, 10%, 15%, 20%, and 30% mass fractions of ZnO were prepared as films and tested in the sensor. The output voltage peaks are shown in Fig. 7.

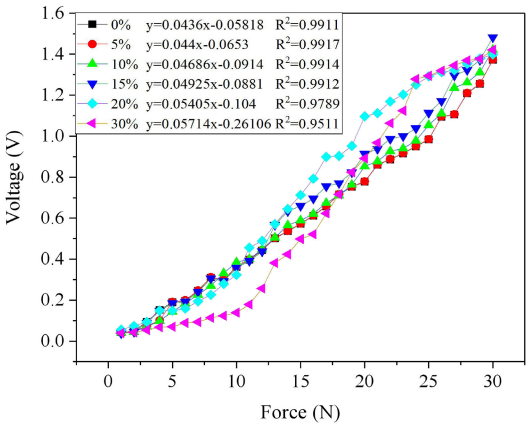

FIGURE 7. Output voltages of the sensors with the PDMS film or the PDMS-ZnO film under different pressures.

Fig. 7 shows that irrespective of whether the sensor uses a PDMS film or a PDMS-ZnO film, the output voltage and force have a linear relationship; as the force increases, the output voltage increases. This is because when a small force is initially applied to the sensor, the contact area between the PDMS or PDMS-ZnO film and the PEO film is small, leading to low amount of transferred charge and output voltage. As the force increases, the contact area between the two films increases and the amount of transferred charge increases, resulting in a higher voltage output.

A comparative analysis of PDMS-ZnO films with different concentrations of ZnO indicates that as the concentration of ZnO increases, the nonlinear characteristics of voltage and pressure become more obvious. When the input force is small, the output voltage decreases with increasing ZnO concentration. This is because the piezoelectric effect is not obvious at a small force, and higher ZnO concentration hardens the film, decreasing the corresponding film deformation. As the contact area between the PDMS-ZnO film and the PEO film decreases, the total output voltage decreases. When the input force is large, the contact area between the PDMS-ZnO film and the PEO film increases, the piezoelectric effect is more obvious, and the total output voltage increases. Fig. 7 shows that the 10% PDMS-ZnO thin film has excellent linearity, a linear correlation coefficient R^2 of 0.9914, and sensitivity slightly higher than that of pure PDMS.

TABLE 1. Statistical test results for PDMS-ZnO and PDMS films.

Force	Ave		SD		T	P	95% confidence interval	
	0%	10%	0%	10%			Lower limit	Upper limit
1N	0.0431	0.0412	1.35E-04	2.33E-04	22.33403	1.42E-14	0.00172	0.00208
5N	0.18884	0.1431	1.26E-03	7.36E-04	99.35056	4.07E-26	0.04478	0.04671
10N	0.36206	0.3849	1.45E-03	2.28E-03	-26.74767	6.06E-16	-0.02463	-0.02105
15N	0.57208	0.58981	9.40E-04	3.56E-03	-15.22241	1.01E-11	-0.02017	-0.01528
20N	0.77774	0.85496	2.24E-03	3.03E-03	-64.74386	8.88E-23	-0.07973	-0.07471
25N	0.98406	1.055	4.04E-03	2.86E-03	-45.28659	5.32E-20	-0.07423	-0.06765
30N	1.37503	1.42469	4.88E-03	4.26E-03	-24.23192	3.42E-15	-0.05397	-0.04535

The output voltages of the 10% PDMS-ZnO film and PDMS film under forces of 1, 5, 10, 15, 20, 25, and 30 N were tested with experiments repeated ten times. Further, a T test was performed on the test results of the two samples (Table 1). A P-value considerably less than 0.05 indicates that the characteristics of the PDMS-ZnO film and the PDMS film are different.

C. EFFECT OF FREQUENCY ON OUTPUT VOLTAGE

Under the frequency conditions of 1, 2, 3, and 4 Hz, normal forces of 1, 5, 10, and 15 N were applied to the sensors. The measured output voltage is shown in Fig. 8.

Figs. 8(a)–(d) indicate that under the same external force, the amplitude of the output voltage of the sensor increases with increasing frequency, especially at forces of 1 N and 5 N.This is because under the action of the force with higher frequency, the contact area is larger and the rate at which contact-separation occurs between the PDMS-ZnO and PEO films is faster, resulting in faster charge transfer between the two films. The higher rate of charge transfer increases the output voltage. Under forces of 10 N and 15 N, the changes in the output voltage amplitude at 3 Hz and 4 Hz are not obvious. This is because with increasing applied force, the contact area between the two films increases, and the charge transfer amount tends to saturation. Therefore, the effect of increase in the frequency of the force on the output voltage amplitude of the sensor is not obvious. The test results demonstrate that the sensor determines the frequency of the applied force on the basis of the amplitude-frequency characteristics, as shown in Figs. 8(e)–(h).. It can determine the magnitude of the force according to the relationship between the input force and the output voltage at different frequencies, as shown in Fig. 8(i).

D. NORMAL PRESSURE PERCEPTION

The proposed sensor can sense the pressure magnitude and the duration of contact with the object and can be used for tactile sensing of smart devices. To test this, normal forces of different magnitudes were applied to the sensors for 0.2, 0.5, and 1 s. The experimental results are shown in Fig. 9.

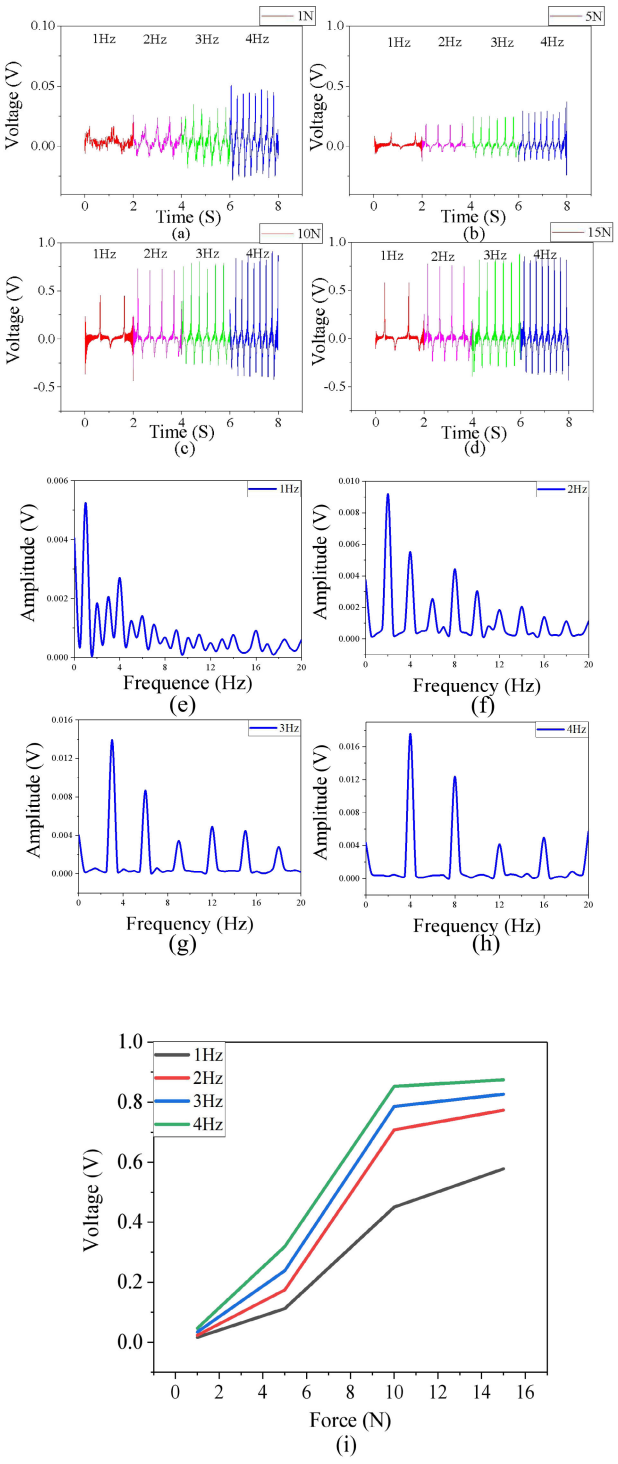

FIGURE 8. Output voltages under a frequency range of 1–4 Hz and normal force of 1 N (a), 5 N (b), 10 N (c), and 15 N (d); amplitude–frequency characteristic curve of the output voltage (e)–(h) and the relationship between force and output voltage (i).

Fig. 9 indicates that under the same force magnitude, the output voltage amplitudes of the sensor are equal. However, the longer the force applied, the longer is the time interval between the peak and trough of the voltage, and the

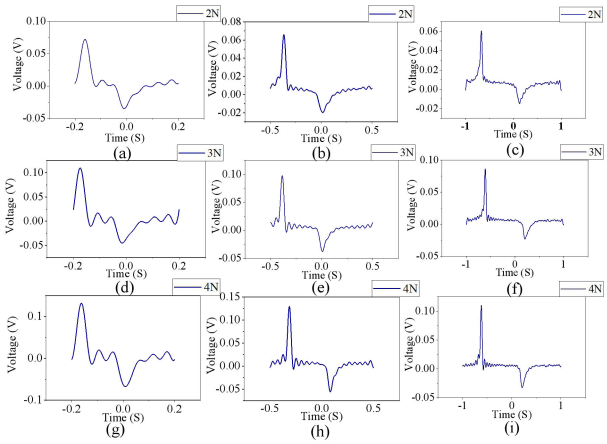

FIGURE 9. Output voltages at a normal force of 2 N applied for 0.2 s (a), 0.5 s (b), and 1 s (c); 3 N applied for 0.2 s (d), 0.5 s (e), and 1 s (f); and 4 N applied for 0.2 s (g), 0.5 s (h), and 1 s (i).

time interval is equal to the duration of the force. This result indicates that the peak output voltage is positively related to the magnitude of the applied force and independent of the duration of the force. This is because the sensor works on the basis of the contact-separation of the PDMS-ZnO film and the PEO film. When an external force is applied on the sensor, the PDMS-ZnO film deforms and contacts the inner PEO film, and charge transfer occurs. A positive voltage is generated on the electrode, leading to a spike in the voltage waveform. Because of the high impedance of the two films, the charge is continuously retained on their surfaces, realizing an electrostatic equilibrium state before the separation of the two films. When the external force is removed, the two charged films are separated from each other, forming an electric field and a negative potential difference between the electrodes; at this time, a trough in output potential is formed. By this process, the sensor can determine the contact and non-contact of external objects with its pressure head on the basis of the output voltage peaks and troughs. The duration of the force can be calculated on the basis of the time difference between the peak and trough of the output voltage.

E. FORCE DIRECTION SENSATION

The sensor can detect not only normal force but also tangential force and determine the direction of the force. The sensor consists of two parts: a hollow cube with an upward opening and a cross beam-shaped pressure head. When a tangential force is applied to the sensor, the middle column tilts toward one side or two adjacent sides of the four sides of the cube. As a result, the PDMS-ZnO and PEO films are pressed, and the sensor outputs the corresponding voltage signals. The magnitude and direction of the tangential force can be determined on the basis of the amplitude of the voltage signals.

A test was conducted to determine the tangential force of 2 N applied on the sensor at angles $\alpha = 0°$–$90°$ with

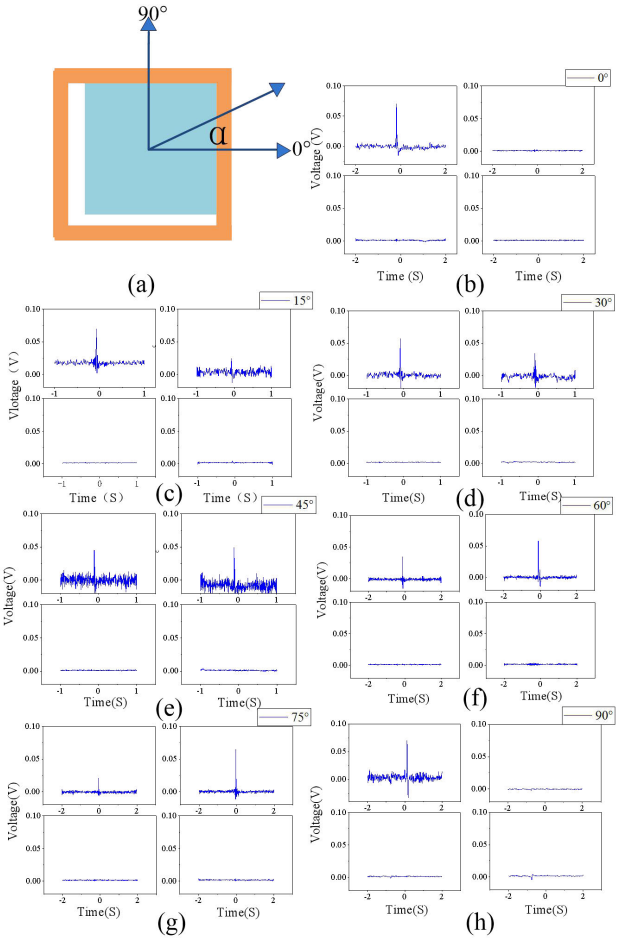

FIGURE 10. Top view of the sensor under tangential force (a), output voltages on the four lateral electrodes of the sensor under tangential forces applied at 0°(b),15° (c), 30° (d), 45° (e), 60° (f), 75° (g), 90° (h).

increments of 15°, as shown in Fig. 10(a). The test results are shown in Figs. 10(b)–(h). The four curves in these figures correspond to the output voltages of the four faces of the sensor. The two surfaces that come in contact in the direction of the applied tangential force output a certain voltage, while the output voltages of the other two surfaces are ignored. The ratio of the voltage peaks of the two adjacent faces is equal to the tangent of the tangential force angle, and there is no phase difference between the output voltage of each face.

The voltage peaks on two adjacent electrodes at different angles are represented by histograms, as shown in Fig. 11. Clearly, the output voltage is larger on the side on which greater pressure is applied. The arc tangent of the peak voltage ratio of the two electrodes is consistent with the tangential force angle. The arc tangent results obtained from the test and calculation, represented by the black and red curves in Fig. 11, respectively are similar. At oblique force angles of 30° and 60°, the relative errors between the measured and calculated values are 0.36% and 1.15%, respectively; the maximum measurement error does not exceed 3°. This is because when the sensor is subjected to a tangential force,

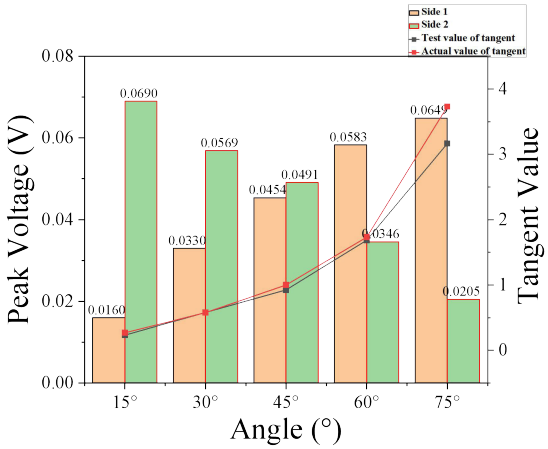

FIGURE 11. Peak voltages of two adjacent electrodes and the arc tangent of the peak voltage ratios.

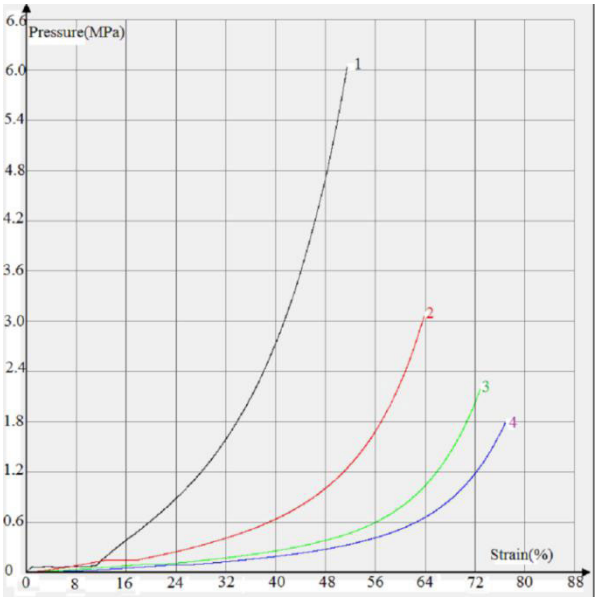

FIGURE 12. Measured pressure and strain curves.

the cross beam in the middle of the sensor is in contact with the inside of the sensor. Moreover, the two adjacent faces of the sensor are squeezed simultaneously, resulting in the thin films on the two faces coming in contact with each other and generating the corresponding output voltage. Because the sensor is a cube, the applied tangential force can be decomposed into a force perpendicular to two adjacent faces, according to the principle of vector synthesis and decomposition of moments. Because forces of the same magnitude are applied at different angles, the forces on the two faces differ, resulting in different contact areas of the films on the two faces, thereby outputting corresponding voltage signals. In addition, because the four faces of the sensor are independent of each other, the tangential force applied on the sensor in one direction causes only two adjacent faces to be pressed, keeping the voltage on the remaining two faces approximately zero.

The elimination of the dimensional coupling between the forward and tangential forces of the sensor enables the sensor to accurately detect multi-dimensional forces and improves the sensor's ability to sense complex input forces.

F. EFFECT OF CONTACT SURFACE HARDNESS

Although this sensor can directly detect a three-dimensional force, when the pressure head of the sensor is covered by an object, the hardness of the object has a significant effect on the sensor output voltage. To test this effect, we prepared cubes of dimensions 10 mm × 10 mm × 5 mm using PDMS solutions at 3%, 5%, 7%, and 10% concentrations. As the concentration of PDMS increases, the hardness increases. To quantify the degree of softness and hardness, an electronic universal testing machine controlled by a microcomputer was used to test the elastic modulus of cubes with different PDMS concentrations. Elastic modulus is a measure of the ability of an object to resist elastic deformation. A force sensor with a range of 100 kN and accuracy of 0.01 N was adopted. The maximum compression force was 320 N. The measured stress and strain curves are shown in Fig. 12, It can be seen from Fig. 12 that before the curve inflection point, the stress and strain are in a linear relationship, and the deformation of the material is proportional to the force, where the ratio of stress to strain is called the elastic modulus. After the inflection point, as the stress increases, the relationship between stress and strain is nonlinear. This inflection point is called the proportional limit point,and the elastic modulus is shown in Fig. 13(a). The figure indicates that as the concentration of PDMS increases, the elastic modulus increases exponentially, and the hardness of the material increases accordingly.

PDMS cubes were then fixed on the pressure head, and the output rod of the vibration modal analyzer was applied vertically on the PDMS cubes with a force of 4 N at 1 Hz. The test results presented in Fig. 13(b) indicate that as the PDMS concentration and elastic modulus increase, the output voltage of the sensor increases. PDMS concentration less than 10% has a linear relationship with the peak output voltage, indicating that an elastomer can reduce the response of the sensor to the external force. Therefore, it is possible to measure a larger input force by installing an elastomer on the pressure head, thus expanding the measurement range of the sensor.

G. SLIDING SENSATION

This sensor not only senses the contact position as well as the magnitude and direction of the contact force but also can detect the sliding of objects. When a manipulator grips an object, especially a flexible object, it needs to use a minimum clamping force to stably grasp the object. The object is subject to an upward static friction force to overcome the effect of gravity to keep the object stationary. If the static friction force on the surface of the object is less than gravity, the object will

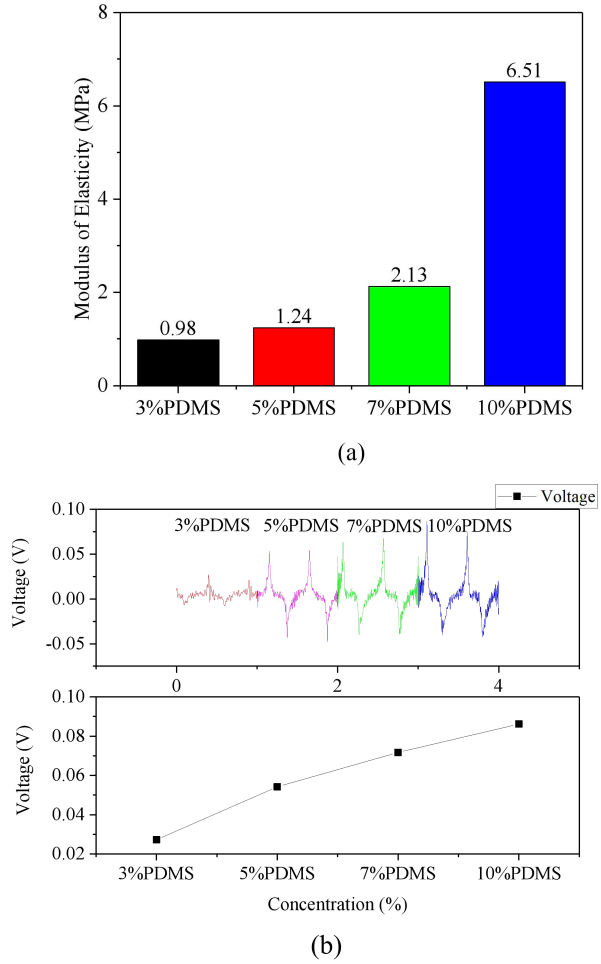

FIGURE 13. Elastic modulus (a); the relationship between the PDMS concentration and output voltage (b).

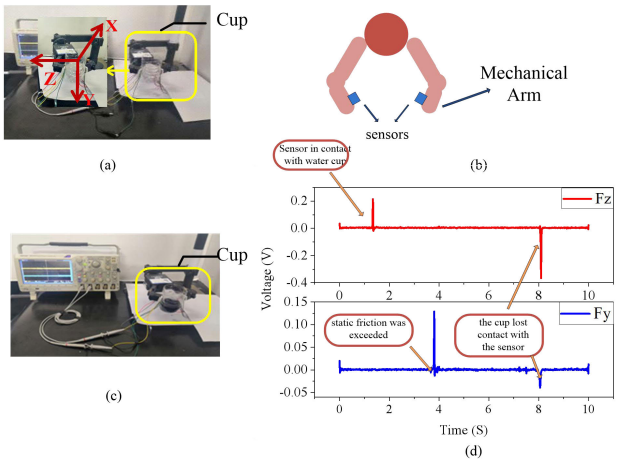

FIGURE 14. Installation position of the sensor in the manipulator and the coordinate system (a); illustration of the installation position of the sensor on the manipulator (b); injection of ink to the plastic cup for testing (c); the output voltage of the sensor during the sliding process of the water cup (d).

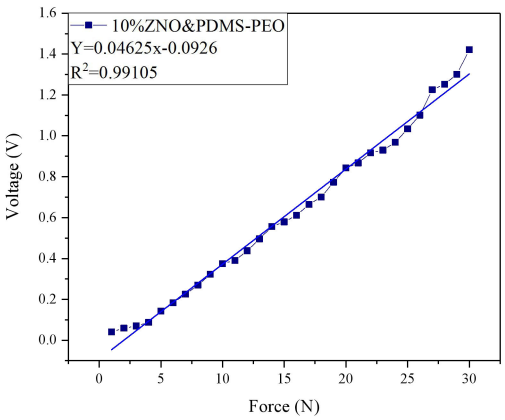

FIGURE 15. Linear relationship between output voltage and force of sensor after repeated experiment.

slide downward, causing sliding friction with the manipulator, and the object will be subject to upward dynamic friction. The relative movement between the object and the sensor installed in the manipulator will exert a downward force on the sensor's pressure head, causing it to bend downward and squeeze the inside of the sensor, thereby generating a voltage change in the electrodes. To test the sensor's perception of sliding, we used a manipulator to clamp a water cup weighing 27.19g. Blue ink was added to the water in the cup for easy identification. First, the sensor was fixed to the manipulator, and the manipulator was made to grasp an empty plastic water cup, which was controlled by a host computer (Fig. 14(a)). Fig. 14(b) shows the installation position of the sensor. At this time, the sensor received pressure in the Z direction. Blue ink was gradually injected into the water cup by a fluid pump at a rate of 0.04 L/s. (Fig. 14(c)). The gravity of the water cup gradually increased and exceeded the static friction force at 3.8 s, causing the water cup to begin sliding downward, and the weight of the water cup was 123.22 g. The water cup left the manipulator at 8.2 s, and at this time, the weight of the water cup was 299.41 g. A total of 272.2 mL of blue ink was poured into the water cup during the entire test.The output voltage of the sensor measured on the corresponding electrode is shown in Fig. 14(d). The voltage of the electrode in the Z direction clearly records the time when the manipulator was in contact and separated from the water cup, and the electrode voltage in the Y direction indicates the process of the water cup starting to slide and leaving the manipulator. The test results show that the sensor can determine whether the object has slipped and thereby assist the manipulator in adjusting the clamping force.

The experimental results verify that the proposed three-dimensional tactile sensor can sense the magnitude and direction of pressure as well as, the hardness and sliding of the contact object. This sensor has good application prospects in the fields of object grasping and handling.

H. REPEATABILITY TEST

In order to verify the repeatability and reliability of the sensor, it was tested while subjecting it to a thousand impacts. The measured sensitivity and the relationship between the output voltage and input force are shown in Fig. 15. The test result indicates that the linear correlation coefficient R^2 and linear equation of the sensor remained changed. Therefore, the sensor has good reliability and repeatability.

IV. CONCLUSION

We designed a three-dimensional flexible tactile sensor that comprises an open hollow cube, a cross beam-shaped pressure head, and polymer films made of PDMS and PEO. The test results indicated that a PDMS-ZnO composite film is better than a PDMS film. The working principle of the sensor was analyzed using the finite element method. The experimental results demonstrated that this sensor can detect various signals. Both the frequency and amplitude of the applied force affect the output voltage of the sensor. This sensor can not only measure the magnitude and frequency of the input force but also sense the duration of the force. The sensor can detect tangential force and judge the applied direction by calculating the arc tangent of the peak voltage ratio of the two adjacent electrodes. The maximum measurement error did not exceed 3°, and the relative error between the measured and calculated arc tangent values was only 0.36% at 30°. On the basis of the output voltage on different electrodes of the sensor, the sensor can judge the sliding of the object in a manipulator. An elastomer can reduce the response of the sensor to the external force. Thus, the range of the sensor can be extended by adjusting the hardness of the pressure head. The proposed sensor can be widely used in robots and wearable devices. In the future, miniaturization and grid design of sensors will be researched to achieve more complex intelligent tactile sensing.

REFERENCES

[1] Y. Cheng, D. Wu, S. Hao, Y. Jie, X. Cao, N. Wang, and Z. L. Wang, "Highly stretchable triboelectric tactile sensor for electronic skin," *Nano Energy*, vol. 64, Oct. 2019, Art. no. 103907.
[2] Z. Liu, Y. Pan, P. Wu, L. Du, Z. Zhao, and Z. Fang, "A novel capacitive pressure sensor based on non-coplanar comb electrodes," *Sens. Actuators A, Phys.*, vol. 297, Oct. 2019, Art. no. 111525.
[3] K. Li, H. Wei, W. Liu, H. Meng, P. Zhang, and C. Yan, "3D printed stretchable capacitive sensors for highly sensitive tactile and electrochemical sensing," *Nanotechnology*, vol. 29, no. 18, May 2018, Art. no. 185501.
[4] J.-C. Wang, R. Karmakar, Y.-J. Lu, C.-Y. Huang, and K.-C. Wei, "Characterization of piezoresistive PEDOT: PSS pressure sensors with interdigitated and cross-point electrode structures," *Sensors*, vol. 15, no. 1, pp. 818–831, Jan. 2015.
[5] D. Song, X. Li, X.-P. Li, X. Jia, P. Min, and Z.-Z. Yu, "Hollow-structured MXene-PDMS composites as flexible, wearable and highly bendable sensors with wide working range," *J. Colloid Interface Sci.*, vol. 555, pp. 751–758, Nov. 2019.
[6] S. Saha, V. Yauvana, S. Chakraborty, and D. Sanyal, "Synthesis and characterization of polyvinylidene-fluoride (PVDF) nanofiber for application as piezoelectric force sensor," *Mater. Today*, vol. 18, pp. 1450–1458, 2019.
[7] M. I. Tiwana, S. J. Redmond, and N. H. Lovell, "A review of tactile sensing technologies with applications in biomedical engineering," *Sens. Actuators A, Phys.*, vol. 179, pp. 17–31, Jun. 2012.
[8] D.-K. Kim, J.-H. Kim, Y.-T. Kim, M.-S. Kim, Y.-K. Park, and Y.-H. Kwon, "Robot fingertip tactile sensing module with a 3D-curved shape using molding technique," *Sens. Actuators A, Phys.*, vol. 203, pp. 421–429, Dec. 2013.
[9] K. Xu, Y. Lu, T. Yamaguchi, T. Arie, S. Akita, and K. Takei, "Highly precise multifunctional thermal management-based flexible sensing sheets," *ACS Nano*, vol. 13, no. 12, pp. 14348–14356, Nov. 2019.
[10] Y. Wang, X. Wu, D. Mei, L. Zhu, and J. Chen, "Flexible tactile sensor array for distributed tactile sensing and slip detection in robotic hand grasping," *Sens. Actuators A, Phys.*, vol. 297, Oct. 2019, Art. no. 111512.
[11] S. Wang, L. Lin, and Z. L. Wang, "Triboelectric nanogenerators as self-powered active sensors," *Nano Energy*, vol. 11, pp. 436–462, Jan. 2015.
[12] C. Alexi and B. Sarah, "Rapid manufacturing of mechanoreceptive skins for slip detection in robotic grasping," *Adv. Mater. Technol.*, vol. 2, no. 1, 2016, Art. no. 1600188.
[13] J. Yu, X. Hou, M. Cui, S. Zhang, J. He, W. Geng, J. Mu, and X. Chou, "Highly skin-conformal wearable tactile sensor based on piezoelectric-enhanced triboelectric nanogenerator," *Nano Energy*, vol. 64, Oct. 2019, Art. no. 103923.
[14] C. Y. Chen, C. Y. Tsai, M. H. Xu, C. T. Wu, C. Y. Huang, T. H. Lee, and Y. K. Fuh, "A fully encapsulated piezoelectric–triboelectric hybrid nanogenerator for energy harvesting from biomechanical and environmental sources," *Exp. Polym. Lett.*, vol. 13, no. 6, pp. 533–542, 2019.
[15] M. Ma, Z. Zhang, Z. Zhao, Q. Liao, Z. Kang, F. Gao, X. Zhao, and Y. Zhang, "Self-powered flexible antibacterial tactile sensor based on triboelectric-piezoelectric-pyroelectric multi-effect coupling mechanism," *Nano Energy*, vol. 66, Dec. 2019, Art. no. 104105.
[16] J.-I. Lee, S. Pyo, M.-O. Kim, and J. Kim, "Multidirectional flexible force sensors based on confined, self-adjusting carbon nanotube arrays," *Nanotechnology*, vol. 29, no. 5, Feb. 2018, Art. no. 055501.
[17] Z. L. Wang, "Piezoelectric nanogenerators based on zinc oxide nanowire arrays," *Science*, vol. 312, no. 5771, pp. 242–246, Apr. 2006.
[18] F.-R. Fan, Z.-Q. Tian, and Z. L. Wang, "Flexible triboelectric generator," *Nano Energy*, vol. 1, no. 2, pp. 328–334, Mar. 2012.
[19] D. Wang, Y. Lin, D. Hu, P. Jiang, and X. Huang, "Multifunctional 3D-MXene/PDMS nanocomposites for electrical, thermal and triboelectric applications," *Compos. A, Appl. Sci. Manuf.*, vol. 130, Mar. 2020, Art. no. 105754.
[20] P. Ding, J. Chen, U. Farooq, P. Zhao, N. Soin, L. Yu, H. Jin, X. Wang, S. Dong, and J. Luo, "Realizing the potential of polyethylene oxide as new positive tribo-material: Over 40 W/m2 high power flat surface triboelectric nanogenerators," *Nano Energy*, vol. 46, pp. 63–72, Apr. 2018.
[21] L. Lin, Y. Xie, S. Wang, W. Wu, S. Niu, X. Wen, and Z. L. Wang, "Triboelectric active sensor array for self-powered static and dynamic pressure detection and tactile imaging," *ACS Nano*, vol. 7, no. 9, pp. 8266–8274, Sep. 2013.
[22] S. Gao, X. Wu, H. Ma, J. Robertson, and A. Nathan, "Ultrathin multifunctional graphene-PVDF layers for multidimensional touch interactivity for flexible displays," *ACS Appl. Mater. Interfaces*, vol. 9, no. 22, pp. 18410–18416, Jun. 2017.
[23] S. Liu, L. Wang, X. Feng, Z. Wang, Q. Xu, S. Bai, Y. Qin, and Z. L. Wang, "Ultrasensitive 2D ZnO piezotronic transistor array for high resolution tactile imaging," *Adv. Mater.*, vol. 29, no. 16, Apr. 2017, Art. no. 1606346.
[24] U. Khan, T.-H. Kim, H. Ryu, W. Seung, and S.-W. Kim, "Graphene tribotronics for electronic skin and touch screen applications," *Adv. Mater.*, vol. 29, no. 1, Jan. 2017, Art. no. 1603544.

ZHIHUA WANG received the M.Eng. and Ph.D. degrees from the Hebei University of Technology, Tianjin, China, in 2006 and 2011, respectively. His Ph.D. research was on energy harvesting, which was supported by Bowen Wang. Since 2006, he has been a member of the Electrical School, Hebei University of Technology. He has engineering experience in tunnel lighting system design, industrial data collection, and control system design. From January 2006 to January 2007, he conducted a visiting research at the National University of Singapore. His research interests include energy harvesting, flexible sensor, and intelligent control. He was awarded as the Top Young Talent in Hebei Province, China.

SHIMING SUN received the B.S. degree in electrical engineering from the Qingdao University of Science and Technology, Qingdao, China, in 2018. He is currently pursuing the master's degree with the Hebei University of Technology. His research interests include energy harvesting, flexible sensor, and intelligent control.

NA LI received the M.Eng. degree from the Hebei University of Technology, Tianjin, China, in 2011. Her M.Eng. research was on control engineering, which was supported by Tao Liang. Since 2019, she has been a member of the Industrial Technology Center, Chengde Petroleum College. She has engineering experience in motor and control system design. Her research interests include electromagnetic computation, motor winding, and intelligent control.

TAO YAO received the B.E. degree from the Taiyuan University of Technology, Shanxi, China, in 2001, the M.E. degree in mechanical engineering from the Inner Mongol University of Technology, Huhhot, China, in 2005, and the Ph.D. degree in mechanical engineering from the Hebei University of Technology, Tianjin, China, in 2009. His Ph.D. research was on mechanical design and theory. Since 2006, he has been a member of the School of Mechanical Engineering, Hebei University of Technology. He has engineering experience in energy harvesting and wave energy conversion technology. From October 2008 to January 2011, he conducted a Postdoctoral Research with the Ocean University of China. His research interests include energy harvesting, hydraulic transmission, and control. He has been awarded the Network Evaluation Expert of the National Natural Science Foundation of China.

DIANLI LV received the M.Eng. and Ph.D. degrees from the Hebei University of Technology, Tianjin, China, in 2005 and 2011, respectively. His Ph.D. research was on numerical calculation and optimization of electromagnetic field, which was supported by Youhua Wang. Since 2005, he has been a member of the Electrical School, Hebei University of Technology. He has engineering experience in electric field analysis of transformer main insulation. From April 2014 to April 2020, he did a Postdoctoral Project with the Department of Mechanical Engineering, Hebei University of Technology.